The Chemistry of Atomic Transition-Metal Ions: Insight into Fundamental Aspects of Organometallic Chemistry

P. B. ARMENTROUT*,†

Department of Chemistry, University of Utah, Salt Lake City, Utah 84112

J. L. BEAUCHAMP

Arthur Amos Noyes Laboratory of Chemical Physics,‡ California Institute of Technology, Pasadena, California 91125

Introduction

One of the strengths of organic chemistry is the availability of fundamental information relating to the properties of reactive intermediates and the mechanisms and energetics of organic reactions. These data facilitate the assessment of reaction pathways and thus guide the development of experimental strategies to effect selective chemical transformation in high yield. Similar fundamental information is generally lacking in fields concerned with chemical reactions in which transition-metal centers play a seminal role (organometallic chemistry, surface science, catalysis), largely because of the relative youth of these fields and the large diversity in metals, ligands, and environments. One means of obtaining this type of fundamental information is to study key species in the gas phase for comparison with condensed-phase studies.

A starting point for discussing gas-phase studies of organometallic reactions is the potential energy surface (PES) diagram for a general oxidative addition reaction, Figure 1. The oxidative addition intermediate III can be formed via a pathway that involves an activation barrier E_a, or a lower energy pathway via a *chemically activated* species I with sufficient internal energy to overcome $E_a' = E_a$. This latter situation obtains if E^* is substantial, which can be the case for coordinatively unsaturated metal centers in reactive electronic configurations and is often the case for *ionic* systems. Further rearrangement of III may lead to the elimination of small molecules and the *exothermic* formation of stable organometallic products. These reactions are *facile* (in the sense that they occur at thermal energies on every encounter) because all intermediates and their interconnecting transition states (TSs) are lower in energy than the reactants. Reagent electronic (E_{el}) or translational (E_T) excitation can promote *endothermic* reactions, the simplest resulting from cleavage of the newly formed bonds in III.

Even for species as simple as atomic transition-metal ions, organometallic transformations usually involve multistep processes. These transformations have been studied with the entire arsenal of experimental techniques developed for the study of ion–molecule chemistry: conventional tandem mass spectrometry, flowing afterglow (FA) techniques, and ion cyclotron resonance (ICR) mass spectrometry and its Fourier transform adaptation (FT-ICR).[1] In this Account, we limit ourselves to those methods in which motion along the reaction coordinate is the key dynamic variable that can be controlled as reactants approach and measured as the products recede. In our laboratories, guided ion beam techniques have been developed and highly refined for studies of the variation of reaction probabilities with E_T. Complementing this work are measurments of product kinetic energy release distributions (KERDs). Whereas KERDs offer a probe of the TS for the last step in a reaction, observed variations in reactivity with E_{el} and E_T can usually be attributed to features in the PES that are encountered in the approach of the reactants toward the first TS. These techniques further complement one another since the initial step in these reactions is often oxidative addition and *rupture* of H–H, C–H, and C–C bonds at the metal center, while the last step involves the reductive elimination of small molecules from transition-metal centers, i.e., the *formation* of H–H, C–H, and C–C bonds.

Experimental Techniques

The guided ion beam tandem mass spectrometer used for these studies at the University of Utah has been described in detail.[2] This instrument produces a beam of ions with a well-defined mass and a kinetic energy that can be varied over a wide range (3–4 orders of magnitude). Ion–molecule reactions occur in a well-defined region and at a pressure low enough that products are the result of *single ion–neutral encounters*. These experiments yield an absolute reaction cross section, $\sigma(E_T)$, a direct measure of the probability of the reaction at E_T. Cross sections are directly related to rate constants by $k(T) = \langle \sigma v \rangle$, where the brackets indicate integration over a Maxwell–Boltzmann distribution of velocities v. The ability of the ion-beam ex-

Peter B. Armentrout was born in Dayton, OH, on March 13, 1953. He received his B.S. degree from Case Western Reserve University and a Ph.D. from Caltech, where he worked with J. L. Beauchamp. After a postdoctoral position at Bell Laboratories in Murray Hill, NJ, he joined the faculty at the University of California at Berkeley. In 1987, he moved to the University of Utah, where he is currently Professor of Chemistry.

Jack Beauchamp is a native of California, born on November 1, 1942. His first experience with research was as an undergraduate at Caltech, where he worked with George Whitesides (then a graduate student with Jack Roberts). He received a Harvard Ph.D. and a Stanford education with John Baldeschwieler in 1967. In the fall of that year, he joined the faculty at Caltech, where he is now Professor of Chemistry.

(1) For excellent reviews on these other aspects of gas-phase organometallic ion chemistry, see: Allison, J. *Prog. Inorg. Chem.* Lippard, S. J., Ed.; 1986, *34*, 627. Squires, R. R. *Chem. Rev.* 1987, *87*, 623. Freiser, B. S. *Talanta* 1985, *32*, 697. Schwartz, H. *Acc. Chem. Res.* 1989, *22*, 282. The field is also nicely represented in the following recent book: *Gas Phase Inorganic Chemistry*; Russell, D. H., Ed.; Plenum: New York, 1989.
(2) Ervin, K. M.; Armentrout, P. B. *J. Chem. Phys.* 1985, *83*, 166.

Table I
Transition-Metal Bond Dissociation Energies[a]

M	M^+–H	M^+–CH_3	M^+–$(CH_3)_2$	M^+–CH_2	M^+–CH	M–CH_3	M–H
Sc	57 (2)	59 (3)	116 (2)	98 (5)	weak	32 (7)	48 (4)*
Ti	54 (3)	54 (2)	118 (6)	93 (4)	122 (4)	46 (7)	
V	48 (2)	50 (2)	98 (5)	80 (3)	115 (2)	37 (9)	41 (4)
Cr	32 (2)	30 (2)		54 (2)	75 (8)	41 (7)	41 (3)*
Mn	48 (3)	51 (2)		71 (3)		30 (4)	30 (4)
Fe	50 (2)	58 (2)	>96	83 (4)	101 (7)*	37 (7)	46 (3)
Co	47 (2)	49 (4)	110 (5)	78 (2)	100 (7)*	46 (3)	46 (3)
Ni	40 (2)	45 (2)	>96	75 (2)		55 (3)	58 (3)
Cu	22 (3)	30 (2)		64 (2)		58 (2)	61 (4)
Zn	55 (3)	71 (3)	98 (3)			19 (3)	20 (1)*
Y	62 (1)	59 (1)		95 (3)	weak		
Zr	55 (3)						
Nb	54 (3)			109 (7)*	145 (8)*		
Mo	42 (3)						53 (5)
Ru	41 (3)	54 (5)					56 (5)
Rh	36 (3)	47 (5)		91 (5)*	102 (7)*		59 (5)
Pd	47 (3)	59 (5)					56 (6)
Ag	16 (3)						54 (3)*

[a] Kilocalories per mole. Values are at 300 K with uncertainties in parentheses. Values derived from work other than ion beam or KERD data are marked by an asterisk. Original citations for all work may be found in ref 7 and 12.
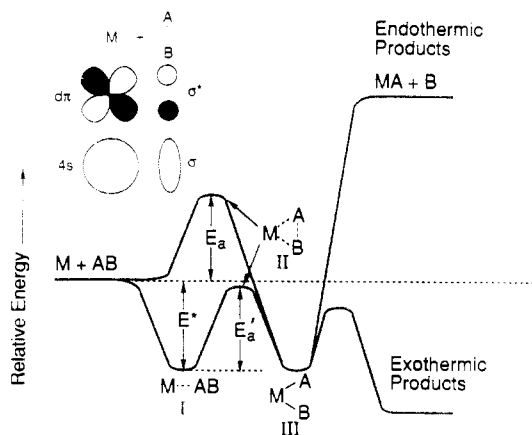

Figure 1. Potential energy surface for a general oxidative addition reaction of a molecule AB to an atomic metal site M. The inset shows the dominant molecular orbital interaction required for the addition process.

periment to measure $\sigma(E_T)$ rather than $k(T)$ is its primary distinguishing feature when compared with FA, ICR, and FT-ICR methods. One advantageous feature of the beam technique is that the ion source is physically separated from the interaction region. This allows tremendous versatility in the means used to produce ions and has enabled us to control the *electronic* energies of transition-metal ions.[3-5]

KERDs were determined by using a reverse-geometry double-focusing mass spectrometer (VG Instruments ZAB-2F) in collaboration with Professor M. T. Bowers at the University of California at Santa Barbara.[6] Atomic metal ions interact with hydrocarbons in the ion source to form adducts, which are accelerated to 8 keV and mass analyzed in the magnetic sector. Ions that decompose in the field-free region between the magnetic and electric sectors are detected by scanning the voltage of the electric sector. The metastable peaks are accu-

mulated and numerically differentiated to obtain the KERDs.

Thermochemistry

During the last several years, we have measured[7] a number of metal–ligand bond dissociation energies (BDEs) and have found them to be in good agreement with available theoretical results.[8] More recently, such thermodynamic results have been obtained via the detailed analysis of KERD data.[6,9,10] Table I summarizes much of the data obtained. As discussed elsewhere,[7] analyses of these values provide *intrinsic* BDEs (the strongest BDE expected in the absence of electronic and steric effects) for MH and MH^+ (57–60 kcal/mol), MCH_3^+ [≃3 kcal/mol > $D°(MH^+)$], MCH_3 [≃3 kcal/mol < $D°(MH)$], MCH_2^+ (≃101 kcal/mol), and MCH^+ (≃130 kcal/mol). We also find that the sum of the two M–C BDEs in $M(CH_3)_2^+$ exceeds typical C–C BDEs of 85–90 kcal/mol, and the sum for $H–M^+–CH_3$ is comparable to typical C–H BDEs of 96–100 kcal/mol. Thus, insertion of M^+ into the C–C and C–H bonds of saturated alkanes is thermodynamically *favorable* in the gas phase.

In relating this gas-phase thermochemistry to condensed-phase species, it is important to realize that gas-phase metal–ligand BDEs *will not equal* the metal–ligand BDE of a saturated metal center. For example, it is unrealistic to expect that the BDE of diatomic CoH or CoH^+ will be equivalent to that for $H–Co(CO)_4$. The relationship between the gas- and condensed-phase thermochemistry is more elusive, but has undergone recent theoretical scrutiny,[11] which establishes that *the intrinsic gas-phase BDEs are useful starting points for*

(3) Elkind, J. L.; Armentrout, P. B. *J. Phys. Chem.* **1985**, *89*, 5626.

(4) Elkind, J. L.; Armentrout, P. B. *J. Phys. Chem.* **1987**, *91*, 2037.

(5) Sanders, L.; Hanton, S.; Weisshaar, J. C. *J. Chem. Phys.* **1987**, *91*, 5145.

(6) Hanratty, M. A.; Beauchamp, J. L.; Illies, A. J.; Bowers, M. T. *J. Am. Chem. Soc.* **1985**, *107*, 1788. Hanratty, M. A.; Beauchamp, J. L.; Illies, A. J.; van Koppen, P.; Bowers, M. T. *J. Am. Chem. Soc.* **1988**, *110*, 1.

(7) Armentrout, P. B.; Georgiadis, R. *Polyhedron* **1988**, *7*, 1573. Armentrout, P. B.; Sunderlin, L. S.; Fisher, E. R. *Inorg. Chem.* ₢ ιbmitted.

(8) Schilling, J. B.; Goddard, W. A.; Beauchamp, J. L. *J. Am. Chem. Soc.* **1986**, *108*, 582; *J. Phys. Chem.* **1987**, *91*, 5616. Pettersson, L. G. M.; Bauschlicher, C. W.; Langhoff, S. R.; Partridge, H. *J. Chem. Phys.* **1987**, *87*, 481.

(9) van Koppen, P. A. M.; Jacobson, D. B.; Illies, A. J.; Bowers, M. T.; Hanratty, M. A.; Beauchamp, J. L. *J. Am. Chem. Soc.* **1989**, *111*, 1991. Deardon, D. V.; Hayashibara, K.; Beauchamp, J. L.; Kirchner, N. J.; van Koppen, P. A. M.; Bowers, M. T. *Ibid.* **1989**, *111*, 2401.

(10) Deardon, D. V. Ph.D. Thesis, Caltech, 1989.

(11) Carter, E. A.; Goddard, W. A. *J. Phys. Chem.* **1988**, *92*, 5679.

Table II
Periodic Trends in Reactivity

	M^+	state	config	s^a	reactant $H_2{}^b$	$CH_4{}^c$	$C_2H_6{}^d$	n-$C_4H_{10}{}^e$
3	Sc^+	^3D	$4s3d$	$^1/_2$	insertion	3–5	6–11	13 (1, 3), 14, 17
	Y^+	^3D	$5s4d$	$^1/_2$	insertion	3–5	6–11	13 (1, 3), 14, 17
4	Ti^+	^4F	$4s3d^2$, $3d^3$	1	insertion	3–5	6–8, 10, 11	13 (1, 2 and 1, 3), 14
5	V^+	^5D	$3d^4$	$1^1/_2$	insertion	3–5	6, 7, 8,* 11	13 (1, 2), 14
	Nb^+	^5D	$3d^4$	$1^1/_2$				14, $-3H_2$
6	Cr^+	^6S	$3d^5$	2	mixed	3–5	6, 7, 11	none
	Mo^+	^6S	$3d^5$	2			8, 10	13
7	Mn^+	^7S	$4s3d^5$	$2^1/_2$	inefficient	4 only	6 only	none
	Fe^+	^6D	$4s3d^6$	2	inefficient	4 only	6, 8, 11 }	13 (1, 4), 15, 16
8	Fe^+*	^4F	$3d^7$	2	direct	4, 5	6, 8,* 11 }	
	Ru^+	^4F	$4d^7$	2		3, 4, RuC^+	6–8, 10	13 (1, 2), 14
9	Co^+	^3F	$3d^8$	$1^1/_2$	direct	4, 5	6, 8,* 11, 12	13 (1, 4), 15, 16
	Rh^+	^3F	$4d^8$	$1^1/_2$	direct		6, 8, 11	13 (1, 2), 14
10	Ni^+	^2D	$3d^9$	1	direct	4, 5	6, 8,* 11, 12	13 (1, 4), 16
	Pd^+	^2D	$4d^9$	1	direct		6	13 (1, 2), 15, 16
11	Cu^+	^1S	$3d^{10}$	$^1/_2$	direct		6, 12	none

^{a} The spin quantum numbers for reactions 2–5. ^{b} The dominant mechanism for reaction of M^+ with H_2. ^{c} This column refers to whether reactions 3–5 are observed. ^{d} This column refers to whether reactions 6–12 are observed. An asterisk indicates that a barrier was observed for a process expected to be exothermic. ^{e} This column indicates whether the exothermic reactions 13–17 are observed. The dominant mode of the dehydrogenation reaction 13 is indicated.

comparison, analysis, and prediction of condensed-phase BDEs.

Reactions with Dihydrogen

The most carefully studied metal reaction system is process 1.[4] This is an ideal system for the investigation of electronic effects in metal ion reactions because it is

$$M^+ + H_2 \rightarrow MH^+ + H \qquad (1)$$
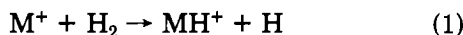
simple (providing an interface with theory) and endothermic (enabling studies of electronically excited metal ions) and isotopes are available (reactions with HD and D_2 provide details concerning reaction dynamics). Our results for reaction 1 indicate that periodic trends in reactivity can be understood by use of molecular orbital (MO) ideas and conservation of spin.[4,12]

Molecular Orbital and Spin Considerations. *Merely having a coordinatively unsaturated metal center is insufficient for efficient bond activation. The electronic requirements at the metal site are more stringent.* Activation of H_2 (or of any covalent single bond) can be viewed as a process in which the bonding electrons of H_2, $\sigma_g(H_2)$, are donated to the metal center, which in turn donates electrons into the antibonding orbital of H_2, $\sigma_u{}^*(H_2)$. Both interactions serve to weaken the H_2 bond while building electron density between the metal and the H atoms. Interactions of H_2 with metal atoms, metal complexes, and metal surfaces have all been discussed theoretically in such terms.[13] For atomic metal ions, the primary acceptor orbital is the s orbital (with contributions from the $d\sigma$), while the donor is a $d\pi$ orbital, leading to the MO interactions displayed in Figure 1. Thus, the atomic metal ion orbital configuration ($s^0 d\pi^2$) should lead directly to formation of ground-state $MH_2{}^+$.[14]

A related consideration in understanding the reactivity of metal ions is spin. Spin is easily conserved

overall in reaction 1 since M^+ can be in either of two spin states and still form ground-state MH^+, as in reaction 2, where the spin quantum numbers of the

$$M^+(s\pm\tfrac{1}{2}) + H_2(0) \rightarrow MH^+(s) + H(\tfrac{1}{2}) \qquad (2)$$

species, Table II, are in parentheses. [For example, ground-state $FeH^+(^5\Delta, s=2) + H(^2S)$ can be formed from both $Fe^+(^6D)$ and $Fe^+(^4F) + H_2(^1\Sigma_g{}^+)$.] However, the favorable $s^0 d\pi^2$ configuration can only be achieved for low-spin ($s - \tfrac{1}{2}$) metal ion states, e.g., $Fe^+(^4F, 3d^7)$. High-spin ($s + \tfrac{1}{2}$) states [resulting from $s^1 d\pi^1$, $d\pi^1 d\pi^1$, etc.; e.g., $Fe^+(^6D, 4s3d^6)$] should have PESs that are more repulsive than those for low-spin states and can only access ground-state intermediates via spin–orbit transitions.

Periodic Trends in Reactivity. Our experimental results for reaction 1 have proven to be a remarkable verification of these ideas. Three categories of reactivity exist based on the electron configuration and spin state of the metal. (1) States such as $Ti^+(^4F, 3d^3)$, Figure 2a, and $V^+(^5D, 3d^4)$ react efficiently with near statistical behavior. The MO concepts indicate that these ions can form a $MH_2{}^+$ intermediate since they can have unoccupied 4s and $3d\sigma$ orbitals. (2) If either the 4s or $3d\sigma$ orbital is occupied and the ion is low-spin, the systems react via a direct reaction mechanism. The behavior of the low-lying excited state $Fe^+(^4F, 3d^7)$, Figure 2b, is typical. (3) If either the 4s or $3d\sigma$ orbital is occupied and the ion is high-spin, the systems react inefficiently, consistent with the repulsive surfaces predicted by the MO concepts. Ground-state $Fe^+(^6D, 4s3d^6)$, Figure 2b, is an example. This categorization for other metal-ion states is summarized in Table II. One proviso here is that mixing of PESs can lead to changes in the expected reactivity. For example, category 3 ions, ground-state $Sc^+(^3D, 4s3d)$ and $Ti^+(^4F, 4s3d^2)$, are observed to react like category 1 ions, $Sc^+(^3F, 3d^2)$ and $Ti^+(^4F, 3d^3)$,[15] because the repulsive ground-state PESs undergo avoided crossings with the attractive excited-state PESs.

(12) Armentrout, P. B. In *Gas Phase Inorganic Chemistry*; Russell, D. H., Ed.; Plenum: New York, 1989; pp 1–42. Armentrout, P. B. In *Molecular Structure and Energetics: C–H Activation*; Liebman, J. F., Greenberg, A., Eds.; VCH: New York. In press.

(13) For example: Saillard, J.; Hoffman, R. *J. Am. Chem. Soc.* **1984**, *106*, 2006.

(14) Rappe, A. K.; Upton, T. H. *J. Chem. Phys.* **1986**, *85*, 4400.

(15) Elkind, J. L.; Armentrout, P. B. *Int. J. Mass Spectrom. Ion Processes* **1988**, *83*, 259. Elkind, J. L.; Sunderlin, L. S.; Armentrout, P. B. *J. Phys. Chem.* **1989**, *93*, 3151.
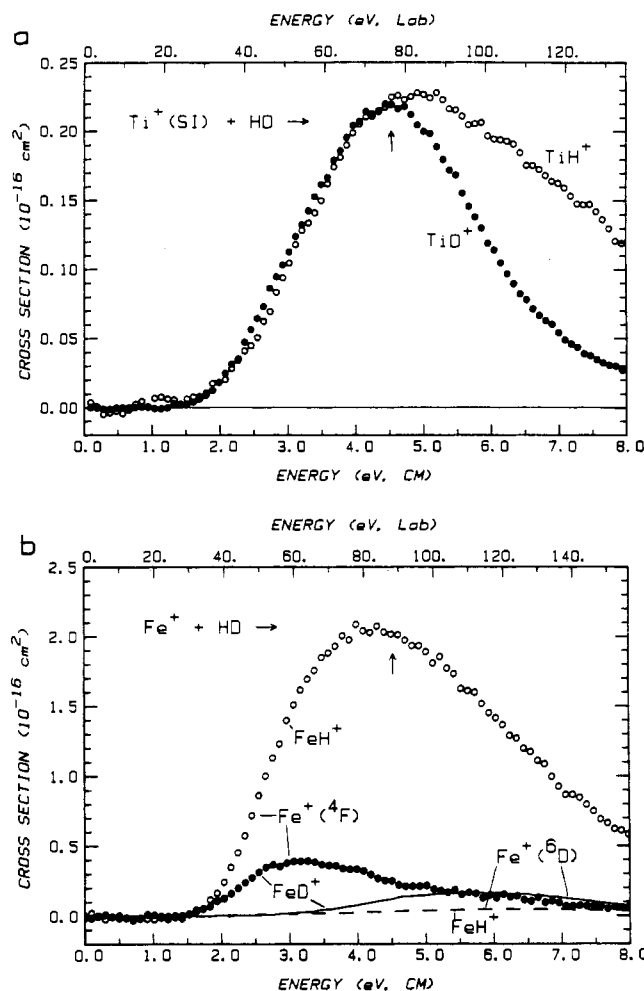
Figure 2. Cross sections for the reaction of (a) Ti^+ and (b) Fe^+ with HD as a function of collision energy in the laboratory (upper scale) and center-of-mass (CM, lower scale) frames. Laboratory collision energies must be converted to CM energies because only the CM energy is available to induce chemical change. The conversion uses the stationary target assumption such that $E_T(CM) = E_T(lab)m/(M + m)$ where m and M are the masses of the neutral and ionic reactants, respectively.

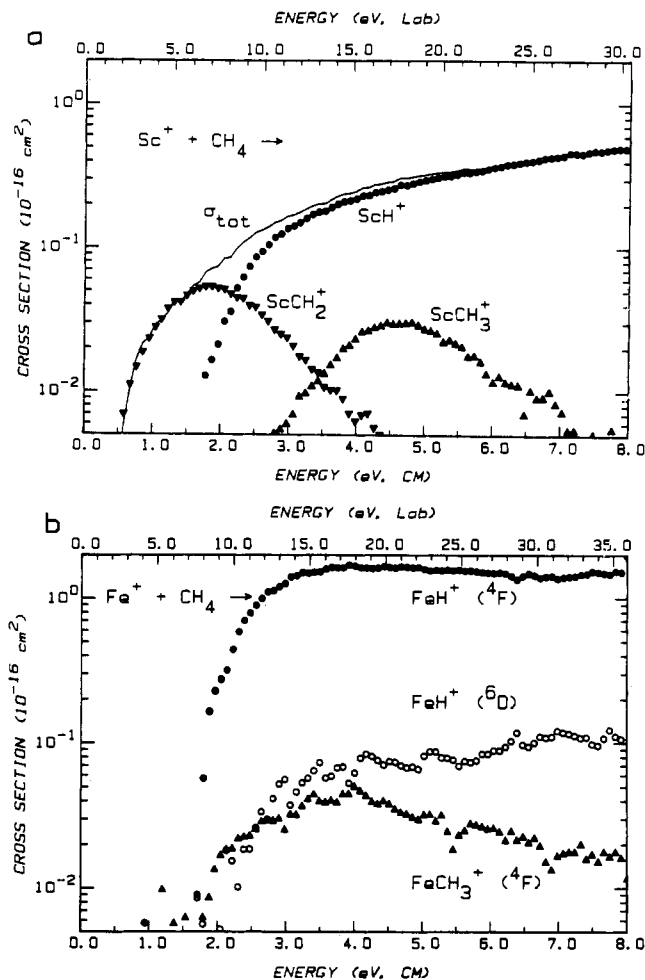## Reactions with Methane and Ethane

A question of obvious interest is whether the electronic considerations important for reaction 1 continue to hold for alkanes. Methane is the simplest system where C–H bond activation can be studied, and ethane extends this to C–C bond activation.

Methane Reactions. Metal ions can react with methane via processes 3–5, where the possible spin quantum numbers are designated. (In the iron exam-

$$M^+(s\pm{}^1/_2) + CH_4(0) \longrightarrow MCH_2^+(s-{}^1/_2) + H_2(0) \quad (3)$$
$$\longrightarrow MH^+(s) + CH_3({}^1/_2) \quad (4)$$
$$\longrightarrow MCH_3^+(s) + H({}^1/_2) \quad (5)$$

ple where $s = 2$, FeH^+ and $FeCH_3^+$ have quintet ground states and $FeCH_2^+$ has a quartet ground state.) State-specific results for reactions of Ti^+, V^+, Cr^+, and Fe^+ with methane indicate that the MO ideas discussed above remain valid for activation of C–H bonds.[12,16,17] The same three categories of reactivity can be differ-

(16) Aristov, N.; Armentrout, P. B. *J. Phys. Chem.* **1987**, *91*, 6178. Sunderlin, L. S.; Armentrout, P. B. *J. Phys. Chem.* **1988**, *92*, 1209. Georgiadis, R.; Armentrout, P. B. *J. Phys. Chem.* **1988**, *92*, 7067.

(17) Schultz, R. H.; Elkind, J. L.; Armentrout, P. B. *J. Am. Chem. Soc.* **1988**, *110*, 411.

Figure 3. Cross sections for the reaction of (a) Sc^+ and (b) Fe^+ with methane as a function of collision energy in the laboratory (upper scale) and center-of-mass (CM, lower scale) frames.

entiated and are summarized in Table II. (1) Reactions 3–5 all take place for Sc^+–Cr^+, Figure 3a, indicative of formation of long-lived intermediates. (2) Species such as $Fe^+(^4F)$, Figure 3b, undergo only reactions 4 and 5, indicating direct processes. (3) Only reaction 4 occurs and it is inefficient as expected for high-spin ions, such as $Fe^+(^6D)$, Figure 3b.

While the general electronic requirements for H_2 and CH_4 activation are similar, the reaction with methane is more sensitive to the spin state of the ion. Dehydrogenation (reaction 3) occurs much more readily (1–2 orders of magnitude) for low-spin metal ion states than for high-spin states.[16] This reaction *requires* a low-spin $(s - {}^1/_2)$ configuration to be spin-allowed, while reactions 2, 4, and 5 do not. However, reaction 3 *is observed* for high-spin metal ions at their thermodynamic limit. These processes must involve a transition between the reactant high-spin PES and the low-spin PES of the intermediates and products. Thus, interactions between surfaces of different spin which were implicated in the H_2 system become obvious in the results for CH_4.

Mechanisms that can explain dehydrogenation of methane at a single metal center are few. The first step is oxidative addition of a C–H bond to the metal center to form H–M^+–CH_3, IV. This intermediate must be in a low-spin state if the M–H and M–CH_3 bonds are covalent, as suggested by theory[18] and experimental
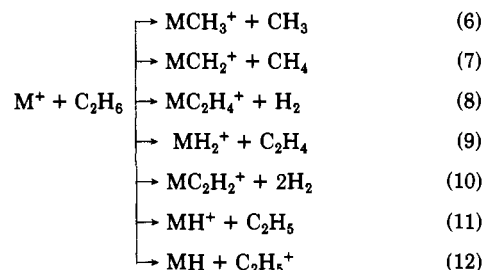
(18) Steigerwald, M. L.; Goddard, W. A. *J. Am. Chem. Soc.* **1984**, *106*, 308.

thermochemistry for M = Sc and V.[7] At low E_T, a four-center symmetry-allowed[18] elimination of H_2 occurs. At higher E_T, IV can decompose by bond fission to form MH^+ or MCH_3^+. Direct reactions form primarily MH^+, which suggests an abstraction (or stripping) reaction proceeding via a collinear M^+-H-CH_3 intermediate.

Ethane Reactions. Observed reactions of atomic metal ions and ethane are processes 6-12. Table II demonstrates that reactivity is highly metal specific.

$$M^+ + C_2H_6 \begin{cases} \rightarrow MCH_3^+ + CH_3 & (6) \\ \rightarrow MCH_2^+ + CH_4 & (7) \\ \rightarrow MC_2H_4^+ + H_2 & (8) \\ \rightarrow MH_2^+ + C_2H_4 & (9) \\ \rightarrow MC_2H_2^+ + 2H_2 & (10) \\ \rightarrow MH^+ + C_2H_5 & (11) \\ \rightarrow MH + C_2H_5^+ & (12) \end{cases}$$

The first two reactions involve C-C bond cleavage. Process 6 is a dominant reaction at high E_T for all metal ions. Reaction 7 is observed only for Sc^+-Cr^+, i.e., the metals in category 1. These processes compete, which suggests that they occur via a common intermediate V, $M(CH_3)_2^+$, which can eliminate CH_4 via a four-center TS or CH_3 via bond fission.

Reactions 8-12 all involve C-H bond cleavage. Reaction 11 or 12 dominates at high E_T for all metal ions. Reaction 8 is not observed for Cr^+, Mn^+, or Cu^+, but is observed for Fe^+, Co^+, and Ni^+, which exhibit a substantial activation barrier even though the reaction is known to be exothermic overall.[17,19] In contrast, Sc^+, Ti^+, V^+, and second-row metal ions show no barrier and large cross sections for reaction 8. As for dehydrogenation of methane, this reaction is much more efficient for low-spin states than for high-spin states of the metal ion.[20] The propensity to activate C-H bonds by the left-side metals is also demonstrated by the observation that only group 3 and 4 metal ions undergo reaction 10 and further by the fact that reaction 9 is observed uniquely for metal ions with two valence electrons, Sc^+, Y^+, La^+, and Lu^+.[21]

These results are generally explained as involving oxidative addition of a C-H bond to the metal center to form $H-M^+-C_2H_5$, VI, which then rearranges to intermediate VII, $(H)_2M^+(C_2H_4)$. Reactions 8 and 9 are explained by reductive elimination of H_2 and competitive ethene loss. Reactions 11 and 12 can occur directly from intermediate VI and depend on the relative ionization energies of MH and C_2H_5. Note that intermediates V and VI are presumably low-spin species since they involve oxidative addition of a covalent C-C or C-H bond just as for IV. Ions in low-spin states can form VI in a spin-allowed process and thus undergo reaction 8 much more efficiently than high-spin states.

Reactions with Larger Alkanes

With larger alkanes, atomic transition-metal ions begin to react in exothermic processes with total cross sections that approach the collision limit, σ_L, several

(19) Georgiadis, R.; Fisher, E. R.; Armentrout, P. B. *J. Am. Chem. Soc.* **1989**, *111*, 4251.

(20) Aristov, N.; Armentrout, P. B. *J. Am. Chem. Soc.* **1986**, *108*, 1806. Sanders, L.; Hanton, S.; Weisshaar, J. C. *J. Phys. Chem.* **1987**, *91*, 5145.
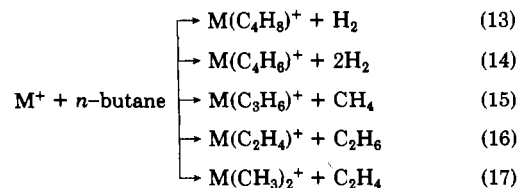
(21) Sunderlin, L. S.; Armentrout, P. B. *J. Am. Chem. Soc.* **1989**, *111*, 3845.
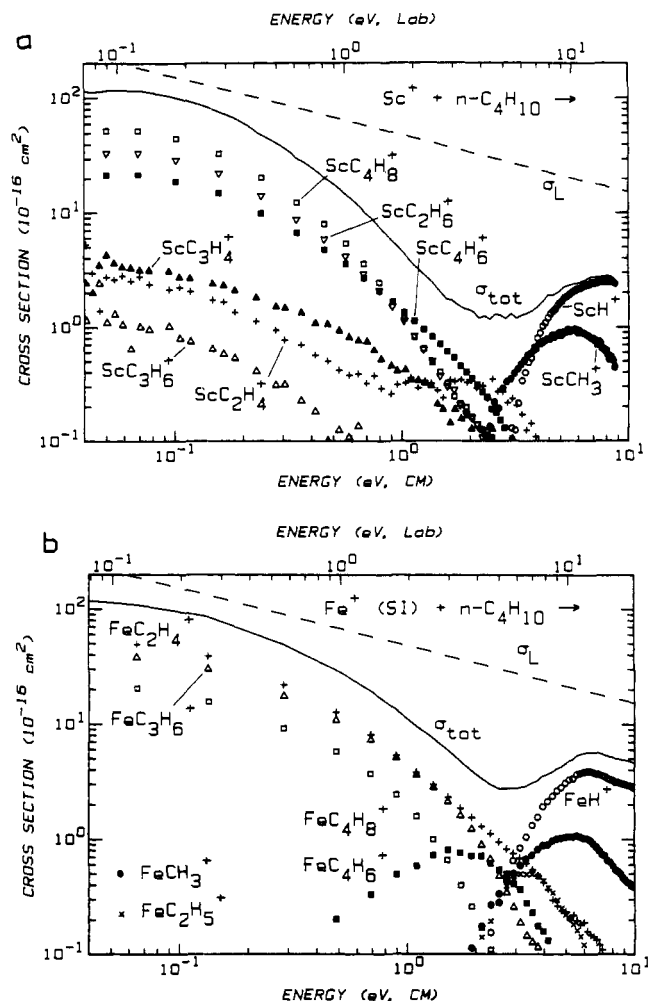
Figure 4. Cross sections for the reaction of (a) Sc^+ and (b) Fe^+ with n-butane as a function of collision energy in the laboratory (upper scale) and center-of-mass (CM, lower scale) frames. σ_L indicates the collision cross section. Fe^+(SI) indicates that the ions, formed by surface ionization, comprise 80% ^6D and 20% ^4F states.

hundred $Å^2$, near thermal energies. This indicates that formation of intermediate III is facile and thermodynamically favorable, i.e., E^* in Figure 1 exceeds E_a' for inserting into C-H and possibly C-C bonds. A further consequence of this attractive PES is that crossings between surfaces of different metal ion states are likely to occur at energies *below* the reactants. The result is extensive interactions among these surfaces (even of different spin) such that the reactions can be largely insensitive to spin.[22]

The major products observed in *exothermic* reactions of metal ions with n-butane, reactions 13-17, are typical of larger hydrocarbons and involve elimination of H_2, small hydrocarbons, and alkenes. The reactivity of

$$M^+ + n\text{-butane} \begin{cases} \rightarrow M(C_4H_8)^+ + H_2 & (13) \\ \rightarrow M(C_4H_6)^+ + 2H_2 & (14) \\ \rightarrow M(C_3H_6)^+ + CH_4 & (15) \\ \rightarrow M(C_2H_4)^+ + C_2H_6 & (16) \\ \rightarrow M(CH_3)_2^+ + C_2H_4 & (17) \end{cases}$$

transition-metal ions can be broadly classified in ac-

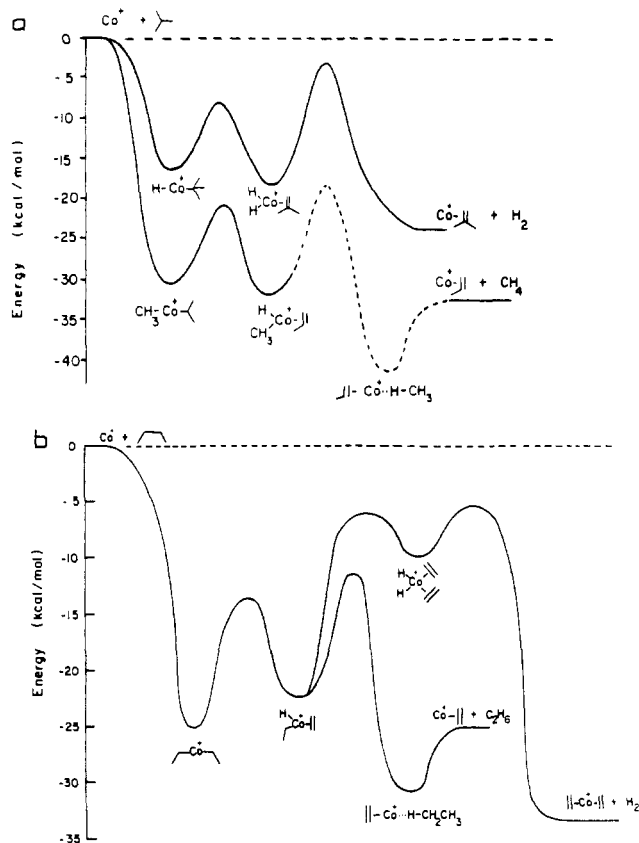(22) This conclusion does not apply to metal ions where the low-spin excited state is very high in energy, e.g., Mn^+, since the crossing point is still well above the reactants' energy.
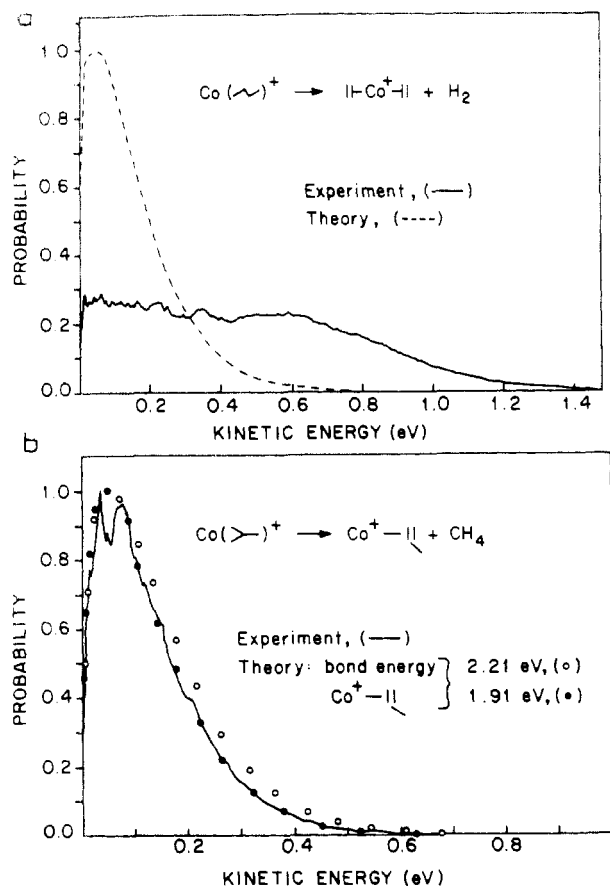
Figure 5. Experimental and theoretical kinetic energy release distributions for (a) loss of H_2 from Co(butane)$^+$ and (b) loss of CH_4 from Co(2-methylpropane)$^+$. The calculated distributions assume no activation barriers for the reverse process. The sensitivity of the fit is shown by two choices for the cobalt ion–propene bond energy.

cordance with the abundance of products for processes 13–17 (Table II). The examples shown in Figure 4 demonstrate that product distributions for exothermic processes are highly metal specific.[23] The first-row group-8–10 metals, typified by Fe$^+$, readily cleave C–H *and* C–C bonds. In contrast, the second-row congeners (Ru$^+$ and Rh$^+$) mainly dehydrogenate hydrocarbons, except that Pd$^+$ behaves more like Ni$^+$. Metals with two valence electrons, Sc$^+$, Y$^+$, La$^+$, and Gd$^+$, are unique in that reaction 17 is prominent.[24] Cr$^+$ and Mn$^+$ are unreactive with hydrocarbons at low E_T, because formation of III requires two relatively strong σ-bonds. For Cr$^+$ and Mn$^+$, the first and second bonds, respectively, are weak due to disruption of a stable half-filled shell. Bonds to Mo$^+$ are slightly stronger, tipping the balance in favor of observing exothermic reactions (Table II).[25]

Classification of reactivity based on product distributions alone can be somewhat misleading. For example, dehydrogenation of *n*-butane (reaction 13) can occur in several specific ways, Table II, as determined by studies with deuterium-labeled alkanes.[24,26] A mechanistically simple and energetically favorable

(23) Beauchamp, J. L. *ACS Symp. Ser.* **1987**, *333*, 11.
(24) Tolbert, M. A.; Beauchamp, J. L. *J. Am. Chem. Soc.* **1984**, *106*, 8117. Schilling, J. B.; Beauchamp, J. L. *J. Am. Chem. Soc.* **1988**, *110*, 15.
(25) Schilling, J. B.; Beauchamp, J. L. *Organometallics* **1988**, *7*, 194.
(26) Tolbert, M. A.; Mandich, M. L.; Halle, L. F.; Beauchamp, J. L. *J. Am. Chem. Soc.* **1986**, *108*, 5675. Halle, L. F.; Houriet, R.; Kappes, M. M.; Staley, R. H.; Beauchamp, J. L. *J. Am. Chem. Soc.* **1982**, *104*, 6293.

Figure 6. Qualitative potential energy diagrams for Co$^+$-induced (a) loss of H_2 and CH_4 from 2-methylpropane and (b) loss of C_2H_6 and H_2 from butane. For simplicity, a chemically activated adduct is not shown in the entrance channel.

pathway is 1,2-elimination to yield M$^+$(2-butene), but early metals remove H_2 in a 1,3 process (presumably yielding a metallocyclobutane product). The 1,4 process has been shown to yield an M$^+$(C_2H_4)$_2$ complex.

Exit Channel Studies

The portion of the PES associated with the *final step* in a complex process falls into two readily distinguishable categories. Type I surfaces are those for which there is no barrier, excluding a centrifugal barrier, to the reverse association reaction (i.e., a "loose" TS). KERDs for such surfaces have been successfully modeled by using statistical theories such as RRKM and phase-space theory (PST). Type II surfaces are those that have a barrier for the reverse association reaction (hence a "tight" TS that involves the simultaneous rupture and formation of several bonds). Rather than being statistical, type II surfaces can lead to a substantial portion of the reverse activation energy appearing as translational energy of the separating fragments. It is usually the *final step of the reaction that determines the KERD*, even when an earlier step may have a higher barrier. Exceptions can occur when early barriers have maxima close to the reactants' energy, in which case they can impose angular momentum constraints which give rise to "cold" distributions.[10]

KERDs for the loss of H_2 and CH_4 from complexes of Co$^+$ with *n*-butane and isobutane, respectively, are shown in Figure 5, along with the best fits of statistical distributions calculated by using PST. The fit is excellent for alkane elimination, which indicates a type I surface. Such a loose TS is depicted in Figure 6 and is consistent with the substantial binding energies

known for stable Lewis acid–base complexes between metal ions and alkanes. In contrast, KERD data for H_2 loss is clearly nonstatistical, demonstrating a type II surface. Further studies also show that, for H_2 loss reactions, both the shape of the distribution and the maximum kinetic energy release are correlated with the reaction mechanism, e.g., 1,2- and 1,4-dehydrogenations are quite distinctive.[6] Such differences suggest that 1,4-elimination dominates the Co^+-induced loss of H_2, HD, and D_2 from $CD_3CH_2CH_2CD_3$. The other isotopic products observed presumably result from scrambling processes, i.e., reversible β-H transfer reactions in Figure 6.

These conclusions regarding the PESs for H_2 and alkane elimination agree with theoretical studies[27] of reductive coupling of H and CH_3 groups from Ni, Pd, and Pt centers. These studies find that the barrier for H_2 elimination is relatively small and "late" with essentially a completely formed H–H bond at the TS. The barrier for elimination of CH_4 is higher and "early", with the M–C and new C–H bonds significantly elongated and the M–H bond still close to the equilibrium length. Such early TSs should allow extensive energy flow from the reaction coordinate into other modes before passage through the loose orbiting TS. In contrast, little energy redistribution is expected for a late TS which is essentially a H_2 molecule associated with a M^+–olefin complex.

Additional information regarding reaction intermediates can be obtained by comparing product branching ratios from the metastable and low-energy ion-beam experiments.[6] For metal–alkane complexes with a fixed internal energy, competitive decomposition reactions from a *common* intermediate will result in similar ratios, while *distinct* noninterconverting structures that decompose at different rates lead to different product yields. For example, product ratios for elimination of H_2 and C_2H_6 from Co^+ and Ni^+ complexes with *n*-butane are similar in both experiments, while the loss of CH_4 is much less abundant in the metastable experiment.[23] These results suggest that CH_4 loss proceeds via an intermediate that decomposes more rapidly than a second intermediate shared by the H_2 and C_2H_6 loss processes (the latter is shown in Figure 6).

Summary and Outlook

It remains a source of frustration to know so much about the reactions of transition-metal ions with hydrocarbons and yet have so many questions remain unanswered. It would be of interest to ascertain whether or not atomic metal ions insert directly into unstrained C–C bonds, since this process has no significant parallels in condensed-phase chemistry. Although implicated by circumstantial evidence and attractive in its simplicity, this process has not been unequivocally substantiated. Considering the difficulty associated with unravelling reactions occurring at a single metal center, it is not surprising that the added complexities introduced by multisite processes have thus far kept reaction mechanisms involving clusters, surfaces, and metal catalysts largely shrouded in mystery. Progress in these various fields may be enhanced by coupling information achieved in all areas.

(27) Low, J. J.; Goddard, W. A. *J. Am. Chem. Soc.* **1984**, *106*, 6928, 8321. Obara, S.; Kitaura, K.; Morokuma, K. *J. Am. Chem. Soc.* **1984**, *106*, 7482.